Propagation of nonlinear reactive contaminants in porous media

Sergio E. Serrano

Civil and Environmental Engineering Department, Temple University, Philadelphia, Pennsylvania, USA

Received 13 December 2002; accepted 24 February 2003; published 30 August 2003.

[1] A study on the effect of nonlinear reactions on the space and time distribution of contaminant plumes governed by the advective-dispersive equation in porous media was conducted. Several models of nonlinear reactions were considered: the irreversible nonlinear first-order kinetic sorption model, the nonlinear Freundlich sorption isotherm model, the nonlinear Langmuir sorption isotherm model, and the reversible nonlinear kinetic sorption model. Each of these models was coupled with the advective-dispersive equation with dimensionless concentration and an approximate analytical series solutions was obtained. Comparison between linear and nonlinear plumes indicated that nonlinear reactions may have a significant effect on the shape and spatial distribution of a contaminant at a given time and in certain cases may explain quantitatively the occurrence of scaled (e.g., concentration change while preserving shape), retarded, and nonsymmetric plumes as well as the presence of back tails and sharp front ends usually observed in the field. By adopting a nonlinear model of contaminant migration a more realistic representation of contaminant propagation is possible than that obtained with a linear model. *INDEX TERMS:* 1832 Hydrology: Groundwater transport; 1829 Hydrology: Groundwater hydrology; 3220 Mathematical Geophysics: Nonlinear dynamics; *KEYWORDS:* Freundlich, Langmuir isotherm, nonlinear, reversible, sorption, groundwater pollution

Citation: Serrano, S. E., Propagation of nonlinear reactive contaminants in porous media, *Water Resour. Res.*, *39*(8), 1228, doi:10.1029/2002WR001922, 2003.

1. Introduction

[2] A common approach to the simulation of transport of reactive contaminants in porous media is to assume that it is governed by an irreversible linear first-order kinetic sorption model, a linear sorption isotherm, or a reversible linear kinetic sorption model [*Fetter*, 1993]. However, studies have revealed that the fate and transport of many contaminants in porous media are sensitive to reaction nonlinearities. It is suspected that nonlinear reactions may have an effect on the shape of the plume, particularly on the phenomenon of long back tails and sharp front ends. Nonlinearity in reactions may be the reason why some contaminant particles arrive at a monitoring point faster, and some slower, than predicted by linear models.

[3] There is a wealth of literature regarding transport through porous media subject to nonlinear equilibrium and nonequilibrium sorption. An excellent summary from the point of view of chemical engineering is given by *Perry and Green* [1997, Chapter 16]. In the area of environmental engineering, several studies have been conducted [*Van Genuchten and Cleary*, 1982; *Bolt*, 1982]. *Weber et al.* [1991] present a review of sorption phenomena, including the effects of nonlinearity on plume shape. They concluded that the center of mass velocity of a contaminant plume that follows a Freundlich isotherm is significantly lower than that of a linear plume when the exponent in the isotherm $b > 1$. The Freundlich plume also exhibits tails that differ from that of the linear sorption plume. Nonlinear sorption is shown to have a strong effect on plume shape. Similar conclusions were found by *Van de Weerd et al.* [1998]. The existence of sharp front ends, enhanced tails, time exponential decrease in plume velocity, and time-linear increase in plume variance was also evidenced in the particle-tracking model of *Abdulaban et al.* [1998].

[4] The hydrologist and the environmental engineer are interested in the forecasting of a plume propagation under nonlinear reactions, given a contamination scenario. From the monitoring, aquifer management, and remediation design points of view, quantitative knowledge of contaminant concentration distribution is desirable. In addition, a mathematical model of plume propagation should be useful in the laboratory estimation of parameters. The prediction of contaminant distribution in time and space may be accomplished by solutions of versions of the mass conservation equation, such as the advective-dispersive equation, subject to a given set of initial, source, and boundary conditions. When the dispersion equation is subject to nonlinear decay, nonlinear sorption or nonlinear reversible reactions, the governing nonlinear differential equation has been solved numerically [e.g., *Sheng and Khaliqb*, 2002; *Boufadel*, 2000]. Analytical solutions of the nonlinear differential equation are difficult. The most important approximate analytical solutions focus on an asymptotic front speed and shape of traveling waves by deriving a traveling wave equation with a moving coordinate system. *Van der Zee* [1990], *Bosma and Van der Zee* [1993], *Simon et al.* [1997], and *Khater et al.* [2002] are representative works with this approach. They concluded that as the magnitude of the nonlinear parameter $b < 1$ decreases there is an increase in front sharpening. Other semianalytical solutions were derived by *Liu et al.*

0043-1397/03/2002WR001922

[2000] using a generalized integral transform coupled with a numerical approximation.

[5] In this article we study the effect of nonlinear reactions on the space and time distribution of contaminant plumes governed by the advective-dispersive equation in porous media. Several models of nonlinear reactions are considered: The irreversible nonlinear first-order kinetic sorption model (section 2); the nonlinear Freundlich sorption isotherm model (section 3); the nonlinear Langmuir sorption isotherm model (section 4); and the reversible nonlinear kinetic sorption model (section 5). Each of these models are coupled with the advective-dispersive equation with dimensionless concentration and an approximate analytical series solutions is obtained. We seek simple and stable approximate analytical solutions that facilitate a comparison with corresponding closed-form solutions to linear equations. We build on the success of the application of decomposition [*Adomian*, 1994] to the solution of nonlinear equations in heterogeneous media without linearization, perturbation, or discretization [*Serrano*, 1995a, 1995b, 1998]. The results are verified with known limited exact solutions and with corresponding finite-difference approximations. Subsequently, simulations are conducted to study the effect of nonlinear reaction parameters on features of contaminant plumes after an instantaneous spill and after an initially symmetric initial condition. Features observed included the magnitude and spatial distribution of contaminant concentration, plume symmetry with respect to its center of mass, and the existence of back tails and sharp front ends. The ultimate aim of this exercise is first the comparison between systems undergoing nonlinear reactions with respect to similar linear ones, and second the building of simple models of groundwater pollution under nonlinear reactions. The latter may prove useful in environmental engineering applications related to parameter estimation, plume forecasting, monitoring, and aquifer restoration. In order to compare nonlinear equations with coefficients dimensionally dependent on the nonlinear parameters with linear ones whose coefficients are independent of such parameters, we cast the equations in terms of dimensionless concentration. This renders the linear and nonlinear equation coefficients dimensionally consistent. With an equal basis for comparison, simulations are conducted and fundamental differences between the linear and nonlinear plumes are noted.

2. Plume Migration Subject to an Irreversible Nonlinear First-Order Kinetic Sorption Model

[6] A common sorption model states that the rate of sorption is a nonlinear function of the concentration of the solute remaining in solution and that once sorbed onto the solid the solute cannot be desorbed. The irreversible first-order kinetic sorption model that describes this is given as

$$\frac{\partial C_s}{\partial t} = k_1 C^b \tag{1}$$

where C_s is the solid-phase contaminant concentration (M/M);$C(x, t)$ is the liquid-phase contaminant concentration (M/L^3); k_1 is a decay constant ($(M/L^3)^{-b}T^{-1}$); b is the nonlinearity factor; and t is time after the spill (T). For an instantaneous point source, the longitudinal contaminant propagation subject to (1) is given by

$$\frac{\partial C}{\partial t} - D\frac{\partial^2 C}{\partial x^2} + u\frac{\partial C}{\partial x} + aC^b = 0, a = \frac{\rho_b k_1}{n}, \quad -\infty < x < \infty, \quad 0 < t$$

$$C(\pm\infty,\ t) = 0, \quad C(x,\ 0) = C_i\delta(x) \tag{2}$$

where D is the aquifer longitudinal dispersion coefficient (L^2/T) assumed constant; u is the aquifer longitudinal pore velocity (L/T) assumed constant; x is longitudinal distance from the source (L); a is the capacity parameter ($(M/L^3)^{1-b}/T$); ρ_b is the soil dry bulk density (M/L^3); n is the soil porosity; C_i is the initial contaminant mass per unit cross-sectional area perpendicular to x (M/L^2); and $\delta(x)$ is the Dirac's delta function.

[7] Defining a dimensionless concentration $c = C/\bar{C}$, with $\bar{C}$ an arbitrary concentration (M/L^3), (2) may be written as

$$\frac{\partial c}{\partial t} - D\frac{\partial^2 c}{\partial x^2} + u\frac{\partial c}{\partial x} + \alpha c^b = 0, \alpha = a\bar{C}^{b-1}, \quad -\infty < x < \infty, \quad 0 < t$$
$$c(\pm\infty, t) = 0,\ c(x, 0) = C_i\delta(x)/\bar{C} \tag{3}$$

where the parameter α has the dimensions of (T^{-1}) regardless of the value of b. This feature of (3) allows the comparison between nonlinear plumes (b $\neq$ 1) with corresponding ones undergoing linear decay ($b = 1$). When $b = 1$ (i.e., linear sorption), the decomposition series of (3) converges to the well known equation (see theorem 2, Appendix B, for proof)

$$c(x,t) = \frac{C_i e^{-\frac{(x-ut)^2}{4Dt} - at}}{\bar{C}\sqrt{4\pi Dt}} \tag{4}$$

When $a = 0$, the solution to (3) reduces to

$$c(x,t) = c_0 = \frac{C_i e^{-\frac{(x-ut)^2}{4Dt}}}{\bar{C}\sqrt{4\pi Dt}} \tag{5}$$

To obtain a solution of (3) when $b \neq 1$, we apply decomposition of the equation in the manner described by *Serrano* [1995a, 1997, 1998], which allows the generation of an analytical series without the need for linearization, perturbation, or discretization. We first define the differential operator $L_t = \partial/\partial t$ and write (3) as

$$L_t c = D\frac{\partial^2 c}{\partial x^2} - u\frac{\partial c}{\partial x} - \alpha N c, \quad NC = c^b \tag{6}$$

or

$$c = DL_t^{-1}\frac{\partial^2 c}{\partial x^2} - uL_t^{-1}\frac{\partial c}{\partial x} - \alpha L_t^{-1} N c \tag{7}$$

where L_t^{-1} is the definite integral from 0 to t. Decomposing c as the infinite series $c = c_0 + c_1 + c_2 + \ldots$, the first term in the series, c_0, satisfies the linear part of (7):

$$c_0 = DL_t^{-1}\frac{\partial^2 c_0}{\partial x^2} - uL_t^{-1}\frac{\partial c_0}{\partial x} \tag{8}$$

To obtain c_0, and using the concept of double decomposition [*Adomian*, 1994], we expand $c_0 = \sum_{m=0}^{\infty} c_{0m}$ in the two terms on the right side of (8). Double decomposition may be used to expand analytically part of the series in order to obtain a simpler expression than would otherwise be obtained, or that could not be obtained, with the complete series. With $c_{00} = C_i\delta(x)/\bar{C}$, the initial condition, (8) becomes

$$c_0 = c_{00} + DL_t^{-1}\frac{\partial^2}{\partial x^2}\sum_{m=0}^{\infty} c_{0m} - uL_t^{-1}\frac{\partial}{\partial x}\sum_{m=0}^{\infty} c_{0m} \tag{9}$$

It is easy to prove that (9) converges to (5), that is to the exact solution to the linear advective-dispersive equation without decay. For the readers not familiar with decomposition, we refer them to theorem 1, Appendix A. Knowing the form of c_0 in (7), we may use a similar procedure to obtain more terms in the series generated by (7). See Appendix C for an introduction to decomposition of nonlinear equations. Thus the nonlinear term in (6) may be expanded as [*Serrano*, 1998, 1995a, 1995b]

$$\begin{aligned} c_1 &= -\alpha L_t^{-1}\sum_{m=0}^{\infty} A_m c_{1m} \\ c_{10} &= c_0 \\ c_{11} &= -\alpha L_t^{-1} c_{10}^b \\ c_{12} &= -\alpha L_t^{-1} b c_{10}^{b-1} c_{11} \\ c_{13} &= -\alpha L_t^{-1}\left(b c_{10}^{b-1} c_{12} + \frac{1}{2}b(b-1)c_{10}^{b-2}c_{11}^2\right) \\ &\vdots \end{aligned} \tag{10}$$

where each term is calculated recursively from the previous ones and the A_m polynomials are given by (C4) (Appendix C) and are specifically applied to the nonlinear operator Nc in (7). Expressing (10) explicitly, we obtain an exponential series of c_0:

$$c(x,t) \approx c_0(x,t)e^{-\frac{2\alpha t c_0(x,t)^{b-1}}{b+1}}, \quad b > 0 \tag{11}$$

where once again c_0 is given by (5) if the initial condition is an instantaneous spill, but in general c_0 is the solution to the linear advective dispersive equation with no decay after a given initial condition. We remark that (11) is not the exact solution of (3) since higher-order terms present in the complete expansion (7) are not included. (11) is called the ''analytic simulant'' of c [*Adomian*, 1994] since it satisfies part of the complete series. In other words, (11) is a truncated series. More terms may be obtained by propagating (11) through the expansion (7). However, (11) is an excellent approximation to the nonlinear solution. We first test (11) with respect to known exact solutions of the advective-dispersive equation. In the absence of decay, $\alpha = 0$ and (11) is identical to the exact solution (5). For the case of linear decay, $b = 1$, and (11) is identical to the exact solution of the exact solution (6). The second set of tests consist in a comparison of the simulant solution (11) with respect to limited numerical solutions to (3). Since an instantaneous point spill is difficult to represent numerically, we consider a numerical solution subject to an arbitrary initial condition. To this end adopt a smooth, symmetric, hypothetical initial condition of the form

$$c(x,0) = \frac{C_i e^{-\frac{x^2}{4}}}{\bar{C}\sqrt{4\pi}} \tag{12}$$

The exact solution to (3) subject to (12) when $b = 1$ (i.e., linear decay) is

$$c(x,t) = \frac{C_i e^{-\frac{(x-ut)^2}{4(1+Dt)} - at}}{\bar{C}\sqrt{4\pi(1+Dt)}} \tag{13}$$

and the exact solution to (3) subject to (12) when $\alpha = 0$ (i.e., no decay) is simply

$$c(x,t) = \frac{C_i e^{-\frac{(x-ut)^2}{4(1+Dt)}}}{\bar{C}\sqrt{4\pi(1+Dt)}} \tag{14}$$

Notice that (14) is also c_0 in (11) when the initial condition is given by (12) instead of an instantaneous spill. Now discretize the spatial domain at fixed intervals $i\Delta x$, $i = 1, 2, \ldots$, and the temporal domain at intervals $j\Delta t$, $j = 1, 2, \ldots$, then a finite-difference solution, c_{ij}, to (3) at nodes i, j might be

$$c_{i,j+1} = c_{i,j} + \frac{\Delta t D}{\Delta x^2}\left(c_{i+1,j} - 2c_{i,j} + c_{i-1,j}\right) - \frac{\Delta t u}{\Delta x}\left(c_{i+1,j} - c_{i,j}\right) - \Delta t \alpha c_{i,j}^b \tag{15}$$

Although (15) is computationally inefficient, it is simple and it serves our purposes.

[8] For the simulations, consider a long aquifer contaminated by an instantaneous point spill with the characteristics: $C_i = 100\ Kg/m^2$, $D = 0.1\ m^2/month$, $u = 0.1\ m/month$, $t = 1\ month$, $b = 0.6$, $\rho_b = 1000\ Kg/m^3$, $n = 0.1$, $k_1 = 10^{-4}\ (Kg/m^3)^{-b}/month$, and $\bar{C} = 1\ Kg/m^3$. Figure 1 shows a comparison of dimensionless concentration, c, versus distance represented by a nondecaying plume (14), a linearly decaying plume (13), a nonlinearly decaying plume (11), and a nonlinear plume according to (15), respectively. Generally, (11) appears to be in reasonable agreement with the finite-difference solution. The shape of the plume tails, the location of the plume center of mass, and the plume variance appears to be accurately predicted. Thus (11) is a useful, simple, and stable expression for practical applications in the forecasting of contaminant propagation, or for parameter estimation, under nonlinear decay during early or prolonged-time simulations and a full range of values in the physical parameters.

[9] The effect of nonlinear decay is one that scales down the concentration profile with respect to the no decay plume, the degree of which is substantially controlled by the magnitude of b. However, there are other subtle but very interesting implications of nonlinearity. In Figure 1 the nonlinear plume is subject to a nonlinear parameter $b < 1$ and dimensionless concentration values are much greater than 1.When this occurs, the nonlinear plume at a given time has a shape located in between the no decay and that of the linear decay plumes. In other words, when $c > 1$ and $b < 1$ the nonlinear plume is scaled up with respect to the

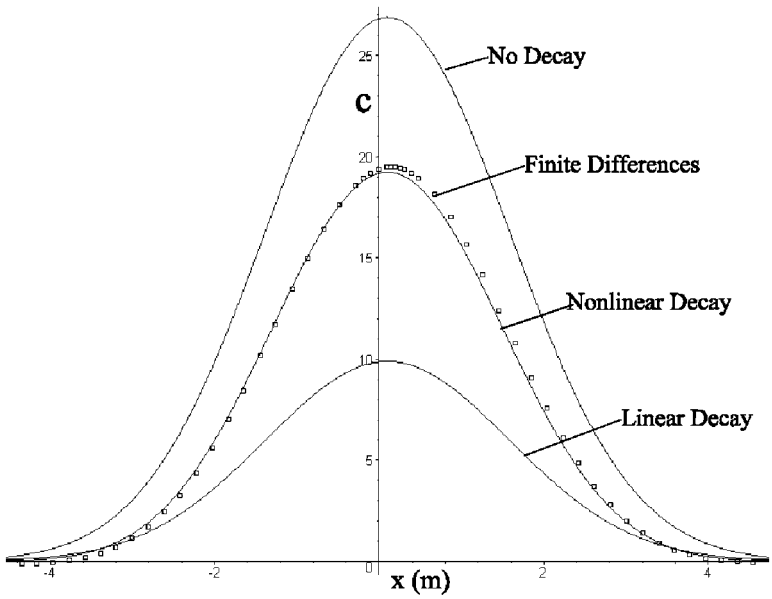

Figure 1. Effect of nonlinear decay on contaminant plume.

linear plume. This situation is illustrated in Figure 2, which shows the relationship between mobile (c) and immobile (c_s) phases for various values of b. The case modeled in Figure 1 corresponds to one of the convex curves in the region $c > 1$ in Figure 2. Within this region, contaminant particles governed by a nonlinear plume experience greater mobility (i.e., less decay) than that of a plume subject to linear decay with $b = 1$. However, for low concentrations, such as those in the plume tales, the opposite is true. In other words, when $c < 1$, and again $b < 1$, the nonlinear plume exhibits less mobility (i.e., more decay) than that of a linear plume and the resulting nonlinear plume is scaled down with respect to that of the linear decay.

[10] On the other hand, it is theoretically possible that $b > 1$, which would correspond to one of the concave curves in Figure 2. The direction of plume scaling is precisely the reverse of that when $b < 1$. In other words, when $c > 1$ and $b > 1$, the nonlinear plume at a given time is scaled down with respect to the linear plume, whereas when $c < 1$ and again $b > 1$, the nonlinear plume is scaled up with respect the linear one. Most plumes have regions with low concentrations in the tails as well as high concentrations in the crest. These intuitive, but dual, implications of the nonlinear theory are well modeled by (11). Figure 3 summarizes the foregoing features of nonlinear plumes. It compares two nonlinear plumes with $b = 0.5$ and $b = 1.5$, respectively, with the corresponding linear. Figure 3 was produced with the same parameter values as Figure 1, except that $u = 1$ *m*/*month*, D = 1 m^2/*month*, and the initial contaminant strength was brought to the vicinity of 1 to

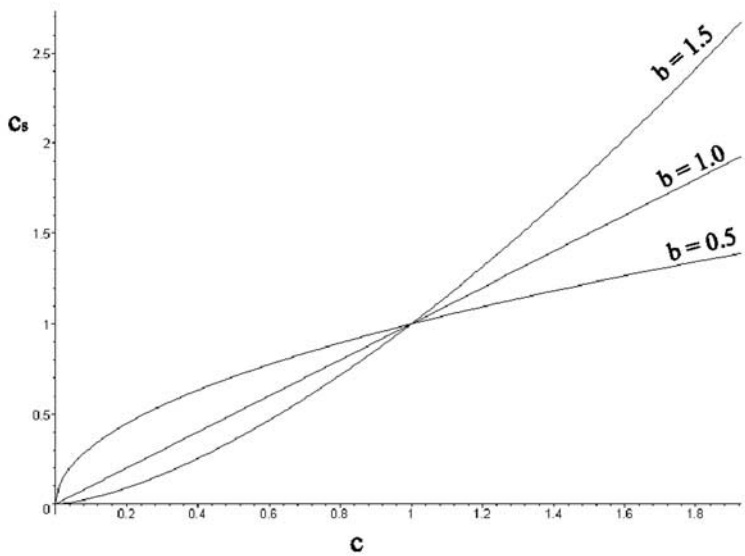

Figure 2. Nonlinear isotherms for various values of b.

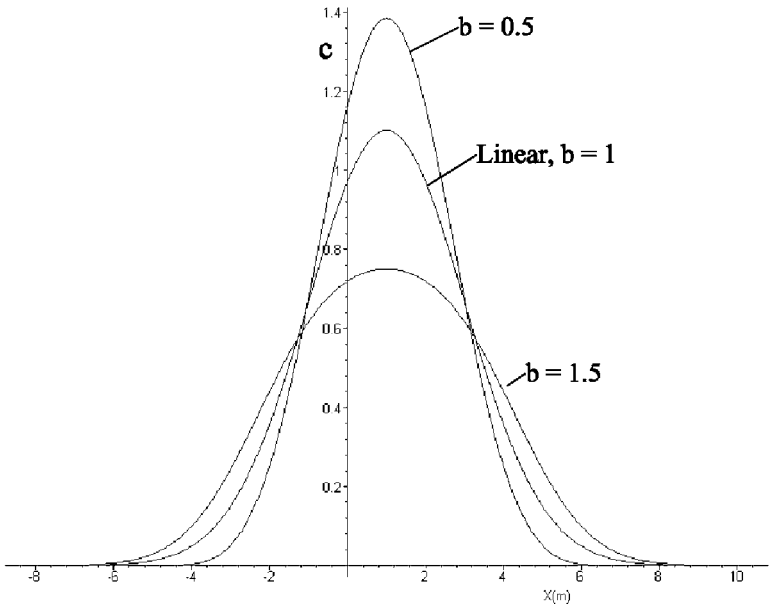

Figure 3. Effect of nonlinear parameter b for various concentration regions.

observe the dual scaling, that is $C_i = 1.5\ Kg/m^2$. Thus we observe that the shape and the direction of scaling of a nonlinearly decaying plume is substantially controlled by the magnitude of b in relation to c. Note that while the tails of one of the plumes experiences scaling in a particular direction, its crest does it in the opposite direction.

3. Plume Migration Subject to Nonlinear Freundlich Sorption Isotherm

[11] Consider the case of contaminant dispersion in a long aquifer subject to a general nonlinear Freundlich isotherm of the form [*Fetter*, 1993]

$$C_s = K_F C^b \tag{16}$$

where K_F is the Freundlich capacity parameter $((M/L^3)^{-b})$; and b is the site energy heterogeneity factor or nonlinearity factor. If $b = 1$, $K_F = K_d$ the linear distribution coefficient. The advective-dispersive equation subject to nonlinear sorption becomes

$$\frac{\partial C}{\partial t} - D\frac{\partial^2 C}{\partial x^2} + u\frac{\partial C}{\partial x} + rbC^{b-1}\frac{\partial C}{\partial t} = 0, \quad r = \frac{\rho_b K_f}{n} \tag{17}$$

subject to the same boundary and initial conditions as (2). As before, we write (17) in terms of dimensionless concentration as

$$\frac{\partial c}{\partial t} - D\frac{\partial^2 c}{\partial x^2} + u\frac{\partial c}{\partial x} + \gamma c^{b-1}\frac{\partial c}{\partial t} = 0, \quad \gamma = rb\overline{C}^{\,b-1} \tag{18}$$

subject to the same boundary and initial conditions as (3). To obtain a solution to (18) we follow a path similar to that for (3). We first write it as

$$c = DL_t^{-1}\frac{\partial^2 c}{\partial x^2} - uL_t^{-1}\frac{\partial c}{\partial x} - \gamma L_t^{-1} Nc\frac{\partial c}{\partial t}, \quad Nc = c^{b-1} \tag{19}$$

With the expansion $c = c_0 + c_1 + c_2 + \ldots$, and knowing that c_0 is given by (5) when the initial condition is an instantaneous spill (see theorem 1, Appendix A), or by (14) when the initial condition is given by (12), we expand the nonlinear term in (19) as

$$\begin{aligned}
c_1 &= -\gamma L_t^{-1}\sum_{j=1}^{\infty} c_{1j}\frac{\partial}{\partial t}\sum_{m=1}^{\infty} c_m \\
c_{10} &= c_0 \\
c_{11} &= -\gamma L_t^{-1} c_{10}^{b-1} \\
c_{12} &= -\gamma L_t^{-1}(b-1)c_{10}^{b-2}c_{11} \\
c_{13} &= -\gamma L_t^{-1}\left((b-1)c_{10}^{b-2}c_{12} + \frac{1}{2}(b-1)(b-2)c_{10}^{b-3}c_{11}^2\right) \\
&\vdots
\end{aligned} \tag{20}$$

Collecting similar terms, and using a slight modification of theorem 1, Appendix A, we arrive at the following simple closed-form expression for the first terms in the series:

$$c(x,t) \approx \frac{C_i e^{-\frac{\left(x - u\phi(x,t/2)\right)^2}{4D\phi(x,t/2)}}}{\overline{C}\sqrt{4\pi D\phi(x,t/2)}}, \phi(x,t) = \frac{t}{\left(1 + \gamma c_0(x,t)^{b-1}\right)} \tag{21}$$

where $2D\phi(x, t)$ is the spatially distributed, time-dependent, plume variance, and ϕ is evaluated at time $t/2$. Again we remark that (21) is the "analytic simulant" of (18), not the exact solution, since it does not contain higher-order terms in the series generated by (19) and (20). However, (21) is close to the exact solution. We tested (21) in a manner similar to the decay equation in the previous section, first

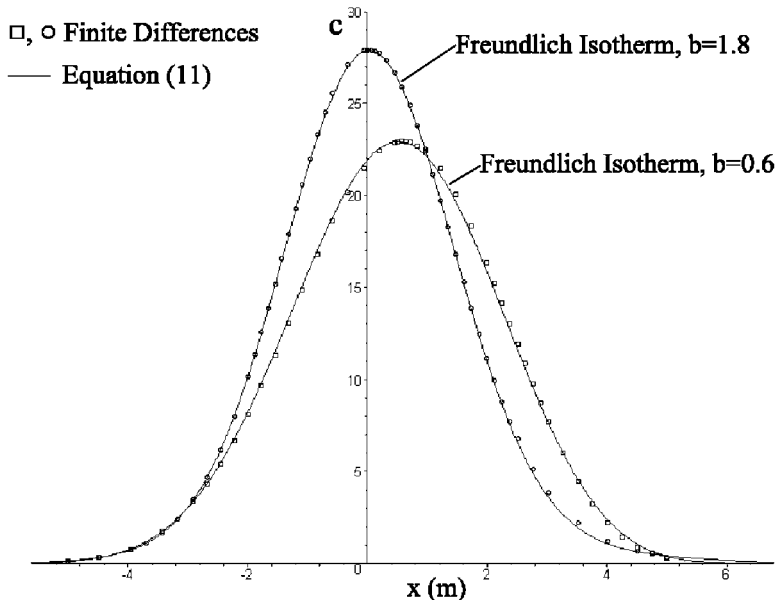

Figure 4. Comparison between solution (21) and finite differences.

with respect to known analytical solutions. For the case of no sorption, $b = 0$ or $K_F = 0$ and (21) is identical to the exact solution (5) of the linear advective-dispersion equation with no sorption. For the case of linear sorption, $b = 1$, $\phi(x, t)$ becomes t/R, where $R = 1 + rb$ the retardation factor of linear sorption, and (21) is identical to the exact solution of the advective-dispersive equation with constant retardation given by (point source)

$$c(x,t) = \frac{C_i e^{\frac{(x-ut/R)^2}{4Dt/R}}}{\bar{C}\sqrt{4\pi Dt/R}} \tag{22}$$

We also tested (21) with respect to a finite-difference solution to (18) in a manner similar to that of the nonlinear decay equation. As an illustration, consider the chemical spill of section 2 (Figure 1), but instead of decay assume the contaminant is subject to sorption that fits a highly nonlinear Freundlich isotherm with $K_f = 10^{-4}$ $(Kg/m^3)^{-b}$. Assume $\rho_b = 1000$ Kg/m^3, $t = 6$ months, and the rest of the parameters as before. Using initial condition (12), Figure 4 shows a comparison between equation (21) with two values of b, one less than one and one greater than 1, and the corresponding finite-difference solutions. In general there is a reasonably good agreement between the two solutions.

[12] Figure 5 shows the spatial distribution of nonlinear plumes, as compared to linear ones when the initial condition is an instantaneous point source, $t = 30$ *months*, $C_i = 10000$ Kg/m^2, and $K_f = 10^{-3}$ $(Kg/m^3)^{-b}$, while keeping the rest of the parameters as in Figure 4. The linear sorption plume was simulated by (22).The no sorption plume was simulated by (5), and the nonlinear plume by (21). Notice

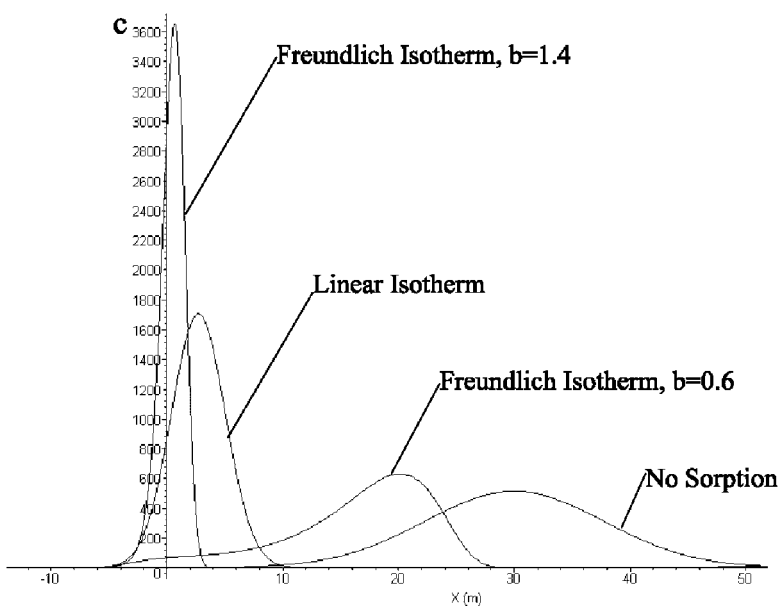

Figure 5. Simulations on the effect of nonlinear Freundlich isotherms.

the nonsymmetric features of the nonlinear plume often reported in the literature [*Van de Weerd et al.*, 1998]: prolonged back tails accompanied by sharp front ends. It was also found that (21) exhibit unusual tails for low values of the dimensionless concentration, c. At this stage of the research we are unable to assess whether this is an instability problem, which is easily corrected by adjusting the value of $\bar{C}$, or due to the special features of nonlinear isotherms in the vicinity of $c = 1$, as described in section 2. These same features appear in plumes subject to the nonlinear Freundlich isotherm: when $b < 1$ and $c > 1$ the nonlinear plume suffers retardation of the processes of advection and dispersion, but not as severe as that of the linear sorption plume. This retardation reduces the velocity of the plume center of mass and the plume variance, the degree of which is controlled by the magnitude of b. The same observations related to nonlinear decay in the previous section are applicable here: Observing the Freundlich isotherm with $b < 1$ in Figure 2, portions of the nonlinear plume with $c > 1$ suffer less sorption (i.e., less retardation, or more mobility) than that of the linear plume. Conversely, portions of the nonlinear plume with $c < 1$ suffer more sorption (i.e., more retardation, or less mobility) than that of the linear plume. Figure 5 also shows that when $b > 1$ and $c > 1$ the nonlinear plume suffers retardation of the processes of advection and dispersion that are more pronounced than that of the linear. This occurs because in this region of the isotherm the nonlinear plume suffers more sorption than that of the linear plume (see Figure 2). This results concur with the conclusions of *Weber et al.* [1991, Figure 24, p. 525] who showed the case of a nonlinear Freundlich isotherm with a parameter $b > 1$ and concentrations $c > 1$: the time-breakthrough concentration curve showed the linear plume arriving much earlier in time than the nonlinear plume, indicating that the nonlinear plume was more retarded than the linear. When $c < 1$, the effect of b on plume shape with respect to the linear plume is expected to be the opposite of that when $c > 1$ as a result of the nonlinear relationship between sorption and concentration. Thus (21) constitutes a simple model that may be used for the forecasting of plume evolution for early or prolonged times, and for the estimation of parameters in column or field experiments. For very high values of t (e.g., $t > 50$ months in this example), (21) becomes unstable at the tails. Extensive simulations indicated that, for very high t, instability is minimized if ϕ in (21) is evaluated at earlier times, for example at $t/4$ instead of $t/2$.

[13] The form of (21) suggests that an equivalent equation representing a nonlinear sorption plume is one with a spatial and temporally variable dispersion coefficient. In concert with these results, many studies in the past proposed theories to describe the scale dependency in the dispersion coefficient of conservative contaminants. For instance, *Serrano* [1996a] attempted to explain the shifting and nonsymmetry of contaminant plumes via a variable dispersion equation responding to evolving heterogeneities at the field scale. These results were obtained after conceiving aquifer heterogeneity in the hydraulic conductivity in stochastic terms. *Serrano* [1995b, 1996b] proposed expressions for the temporal variability in the dispersion coefficient that combined the effects of random heterogeneities with those due to recharge from rainfall and aquifer boundary conditions. *Serrano and Adomian* [1996] proposed equivalent dispersion equations that emphasized the spatial variability in the dispersion coefficient resulting from aquifer heterogeneity and recharge.

[14] An important corollary application of (21) in laboratory tests designed for parameter estimation, is the case of long-column experiments with constant source boundary condition. In this case, the governing equation is (18) subject to a constant concentration, C_0 (M/L^3), at $x = 0$, $0 \le x < \infty$. An analysis similar to that of the instantaneous point source leads to an analytic simulant of the form

$$C \approx \frac{C_0}{2}\left\{erfc\left(\frac{(x - u\phi(x,t/2))}{\sqrt{4D\phi(x,t/2)}}\right) + e^{\frac{ux}{D}} erfc\left(\frac{(x + u\phi(x,t/2))}{\sqrt{4D\phi(x,t/2)}}\right)\right\}, \quad 0 \le x < \infty \tag{23}$$

where $\phi(x, t)$ as in (21), and $erfc(\ )$ denotes the "error function complement." Breakthrough curves of (23) exhibit similar features to nonlinear plumes subject to a point source, except that the concentration on the left boundary remains constant. Again, when $b < 1$ and $c > 1$ the contaminant front of the nonlinear plume is substantially delayed, but not as much as that of the linear sorption plume. Similarly, nonlinear plumes are nonsymmetric with respect to the center of mass, resulting in a front sharper than that of the no sorption plume, but not as much as that of the linear plume. Several previous studies have concluded that as the value of b decreases ($b < 1$) the nonlinear front becomes sharper [i.e., *Van der Zee*, 1990].

4. Plume Migration Subject to Nonlinear Langmuir Sorption Isotherm

[15] Consider now the case of contaminant dispersion in a long aquifer subject to a nonlinear Langmuir isotherm of the form [*Fetter*, 1993]

$$C_s = \frac{\eta\beta C}{1 + \eta C} \tag{24}$$

where η is an absorption constant related to binding energy (L^3/M); and β is the maximum amount of solute that can be absorbed by the solid (M/M). The advective-dispersive equation subject to a Langnuir isotherm becomes

$$\frac{\partial C}{\partial t} - D\frac{\partial^2 C}{\partial x^2} + u\frac{\partial C}{\partial x} + \frac{r_1}{(1 + \eta C)^2}\frac{\partial C}{\partial t} = 0, \quad r_1 = \frac{\rho_b \eta \beta}{n} \tag{25}$$

subject to the same boundary and initial conditions as (2). An interesting feature of the Langmuir model is that eta is a shape, or nonlinearity, parameter, whereas β is a scale parameter. Unlike the Freundlich model, where the dimensions of K_F depend on b, the two parameters of the Langmuir model are not dimensionally related. Therefore the Langmuir model allows the comparison of linear and nonlinear plumes without the need for a dimensional transformation. A decomposition series of (25) may be generated from

$$C = DL_t^{-1}\frac{\partial^2 C}{\partial x^2} - uL_t^{-1}\frac{\partial C}{\partial x} - r_1 L_t^{-1} NC\frac{\partial C}{\partial t}, NC = \frac{1}{(1 + \eta C)^2} \tag{26}$$

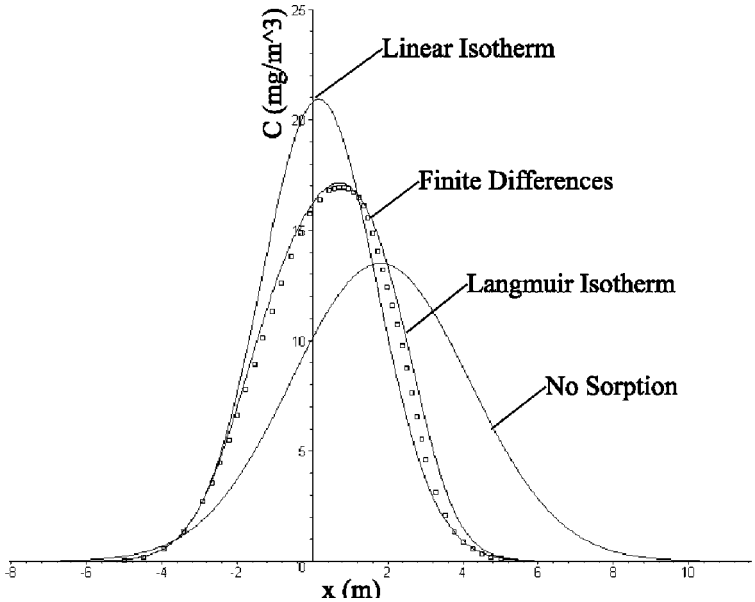

Figure 6. Plume shape under nonlinear Langmuir isotherm.

subject to the same boundary and initial conditions as (3). (26) was subject to the same analysis as described in the previous sections. We omit the lengthy algebraic manipulation necessary for the derivation of the decomposition series, the double decomposition series, and ultimately the analytic simulant. For an instantaneous point source we obtain

$$C(x,t) \approx \frac{C_i e^{-\frac{(x-u\psi(x,t/2))^2}{4D\psi(x,t/2)}}}{\sqrt{4\pi D\psi(x,t/2)}}, \psi(x,t) = \frac{t(1+\eta C_0(x,t))^2}{(1+\eta C_0(x,t))^2 + r_1},$$
$$C_0(x,t) = \bar{C}c_0(x,t) \tag{27}$$

with $\psi(x, t)$ evaluated at a time $t/2$. For a constant left boundary condition, we obtain (23) when $\phi(x, t/2)$ is replaced by $\psi(x, t/2)$, and $\psi(x, t)$ given in (27). When $\eta = 0$ or $\beta = 0$, (27) becomes the solution (5) to the advective-dispersive equation with no sorption. For comparison purposes, an equivalent plume with a linear isotherm would be represented as (27) with $\psi = t/(1 + r_1)$. For the simulations we adopted $\eta = 0.1\ m^3/Kg$, $\beta = 0.01\ Kg/Kg$, $\rho_b = 1000\ Kg/m^3$, $D = 0.1\ m^2/month$, $u = 0.1\ m/month$, $C_i = 80\ Kg/m^2$, $n = 0.1$, $\bar{C} = 1\ Kg/m^3$, and $t = 18$ month. The initial condition was $C(x, 0) = \bar{C}c(x, 0)$ with $c(x, 0)$ given by (12) and $\bar{C} = 1\ Kg/m^3$ as before. Figure 6 shows the concentration spatial distribution for the nonlinear plume, the linear plume, the no sorption plume, and a finite difference solution to (26). As expected, nonlinearity causes a decrease in the velocity of the plume center of mass, and a corresponding increase in the magnitude of the maximum concentration with respect to the no sorption plume. This reduction in the center of mass, and corresponding increase in maximum concentration, is not as drastic as that of the linear plume. As η increases in value, there is more sorption at low concentrations. This phenomenon can be inferred intuitively from the observation of a Langmuir isotherm plotted simultaneously with a linear one. The most "retarded", or the least mobile, is the linear one, and the most mobile, or the most dispersive, is the one without sorption. The shape of the plume may be quite sensitive to the size of the nonlinearity. Again as η increases in magnitude there is more sorption at low concentrations.

5. Plume Migration Under a Reversible Kinetic Sorption Model

[16] When the rate of solute sorption is related to the amount that has already been sorbed and the reaction is reversible, then a reversible linear kinetic sorption model may be applicable. We start with the linear case to establish a basis for comparison. The rate of change of concentration in the solid phase is usually expressed as

$$\frac{\partial C_s}{\partial t} = k_1 C - k_2 C_s, \qquad C_s(0) = 0 \tag{28}$$

where, k_1 is the forward rate constant $((M/L^3)T)^{-1}$; k_2 is the backward rate constant (T^{-1}); and a zero initial solid-phase concentration is assumed. The advective-dispersive equation, with dimensionless concentration, subject to (28) and an instantaneous point source is given by

$$\frac{\partial c}{\partial t} - D\frac{\partial^2 c}{\partial x^2} + u\frac{\partial c}{\partial x} + ac - \frac{\omega}{\bar{C}}C_s = 0, a = \frac{\rho_b k_1}{n}, \quad \omega = \frac{\rho_b k_2}{n},$$
$$-\infty < x < \infty, \quad 0 < t \quad c(\pm\infty, t) = 0, \quad c(x,0) = \frac{C_i \delta(x)}{\bar{C}} \tag{29}$$

To solve the coupled equations (28) and (29), we first note that the solution to (28) is the convolution integral

$$C_s = \bar{C}\int_0^t e^{-k_2(t-\tau)} k_1 c(x,\tau) d\tau \tag{30}$$

Substituting (30) into (29) we obtain an integrodifferential equation whose t partial decomposition solution may be obtained from

$$c = DL_t^{-1}\frac{\partial^2 c}{\partial x^2} - uL_t^{-1}\frac{\partial c}{\partial x} - aL_t^{-1}c + \omega k_1 L_t^{-1} \cdot \int_0^t e^{-k_2(t-\tau)} c(x,\tau) d\tau \tag{31}$$

We use the same procedure of section 2, along with Theorem 1 and 2, to obtain an initial term, c_0, for the advective-dispersive operator in (31). The second term in the series generated by (31), c_1, may be expanded as

$$\begin{aligned} c_1 &= ak_2L_t^{-1}\int_0^t e^{-k_2(t-\tau)}\sum_{i=0}^{\infty}c_{1i}(x,\tau)d\tau \\ c_{11} &\approx \frac{a}{k_2}c_0\left(e^{-k_2t}-1\right) \\ c_{12} &= \frac{1}{2}\left(\frac{a}{k_2}\right)^2 c_0\left(e^{-k_2t}-1\right)^2 \\ &\vdots \\ c_{1m} &= \frac{1}{m!}\left(\frac{a}{k_2}\right)^m c_0\left(e^{-k_2t}-1\right)^m \end{aligned} \tag{32}$$

which converges to

$$c_1 = c_0\left(e^{\frac{a}{k_2}\left(e^{-k_2t}-1\right)}-1\right), \quad k_2>0 \tag{33}$$

Thus an approximate solution to (29) or (31) is simply

$$c \approx c_0 e^{\frac{a}{k_2}\left(e^{-k_2t}-1\right)}, \quad k_2>0 \tag{34}$$

as $a \to 0$, (34) reduces to $c_0 = c_0(x, t)$, with c_0 given by (5), that is the no sorption model. As $k_2 \to 0$, (34) approaches to (4), the linear sorption model. Comparison between approximate solution (34) and a finite difference solution indicates reasonable agreement. However, both (34) and the numerical solution disregard a back tail which tends to appear as the values of the backward constant, k_2, increase relative to that of a. A different decomposition solution to (29) that exhibits this tail was obtained. However, this solution involved complex integrals, it was found to be unstable, and it was restricted to large values of k_2. For these reasons it is not presented here. For values of k_2 less than that of a, (34) appears to be a good approximation, although this solution is limited in that it does not show this interesting feature.

[17] Now the nonlinear version of model (28) is

$$\frac{\partial C_s}{\partial t} = k_3C^b - k_4C_s, \quad C_s(0)=0 \tag{35}$$

where, k_3 is the forward rate constant $(M/L^3)^{-b}T^{-1}$and k_4 is the backward rate constant (T^{-1}). The advective-dispersive equation, with dimensionless concentration, subject to (35) and an instantaneous point source is given by

$$\begin{aligned} &\frac{\partial c}{\partial t} - D\frac{\partial^2 c}{\partial x^2} + u\frac{\partial c}{\partial x} + \xi c^b - \frac{\kappa}{\bar{C}}C_s = 0, \xi = \frac{\rho_b k_3 \bar{C}^{b-1}}{n}, \quad \kappa = \frac{\rho_b k_4}{n}, \\ &-\infty < x < \infty, \quad 0 < t \quad c(\pm\infty, t) = 0, \quad c(x,0) = \frac{C_i\delta(x)}{\bar{C}} \end{aligned} \tag{36}$$

Equation (31) now becomes

$$c = DL_t^{-1}\frac{\partial^2 c}{\partial x^2} - uL_t^{-1}\frac{\partial c}{\partial x} - \xi L_t^{-1}c^b + \kappa k_3 L_t^{-1}\int_0^t e^{-k_4(t-\tau)}c(x,\tau)d\tau \tag{37}$$

Combining the decomposition processes of section 2 with those of this section we arrive at a simple approximate solution to (36):

$$c \approx c_0 + c_0^b\left(e^{\frac{\xi}{k_4}\left(e^{-k_4t}-1\right)}-1\right), 0 \le b \le 1, \quad 0 < k_4 \tag{38}$$

As $b \to 1$, (38) reduces to (36), the reversible linear kinetic sorption model. As $\xi \to 0$, (38) reduces to $c_0 = c_0(x, t)$, with c_0 given by (5) or (14), depending on the initial conditions, that is the no sorption model. As $k_4 \to 0$, (38) approaches to the nonlinear sorption model. Equation (38) was also compared with a finite-difference solution to (36), the reversible linear kinetic sorption model (34), the no sorption model (14) when the initial condition is (12), and the irreversible linear sorption model (11). Figure 7 illustrates one such simulation. The following parameter values were used: b = 0.9, t = 1 month, n = 0.1, ρ_b = 1000 Kg/m^3, C_i = 10000 Kg/m^2, k_3 = 10^{-4} $(Kg/m^3)^{-b}month^{-1}$, k_4 = 0.5 $month^{-1}$, $\bar{C}$ = 10000 Kg/m^3, u = 0.1 $m/month$, D = 0.1 $m^2/month$, and the initial condition given by (12). In general the agreement between the numerical solution and (38) is reasonable.

[18] The simulations confirm quantitatively some known features of reversible-reaction models [*Van de Weerd et al.*, 1998]. When there is a time-dependent solid-phase concentration, C_s, the effect of a reversible reaction is that of returning a portion of the contaminant mass to the mobile phase, the degree of which is controlled by the magnitude of the backward constant relative to that of the forward constant. As the magnitude of the backward constant increases, the plume approaches the shape of the corresponding no-sorption one. Conversely, as the magnitude of this constant decreases, the plume approaches the shape of that of the linear sorption plume. If in addition, the forward reaction is nonlinear the shape of the plume may be significantly scaled. As explained in section 2, the degree of plume scaling depends on the magnitude of the nonlinear parameter b. On the other hand, the direction of plume scaling, either up or down, is controlled by the position in which a particular plume region stands in the solid-phase liquid-phase relationship (see Figure 2). Figure 8 shows the effect of different values of the nonlinear parameter b. In these simulations, u = 1 $m/month$, D = 1 $m^2/month$, and $\bar{C}$ = 1 Kg/m^3, and the rest of the parameters are as in Figure 7. Clearly, the effect of nonlinearity, as measured by the magnitude of b, may be substantial. Thus neglecting nonlinearity may simplify the mathematics but may considerably affect the accuracy in the predicted contaminant concentrations.

6. Summary and Conclusions

[19] A study on the effect of nonlinear reactions on the space and time distribution of contaminant plumes governed by the advective-dispersive equation in porous media was conducted. Several models of nonlinear reactions were considered: The irreversible nonlinear first-order kinetic sorption model; the nonlinear Freundlich sorption isotherm model; the nonlinear Langmuir sorption isotherm model; and the reversible nonlinear kinetic sorption model. Each of these models were coupled with the advective-dispersive equation with dimensionless concentration and an approximate analytical series solutions was obtained. The solutions

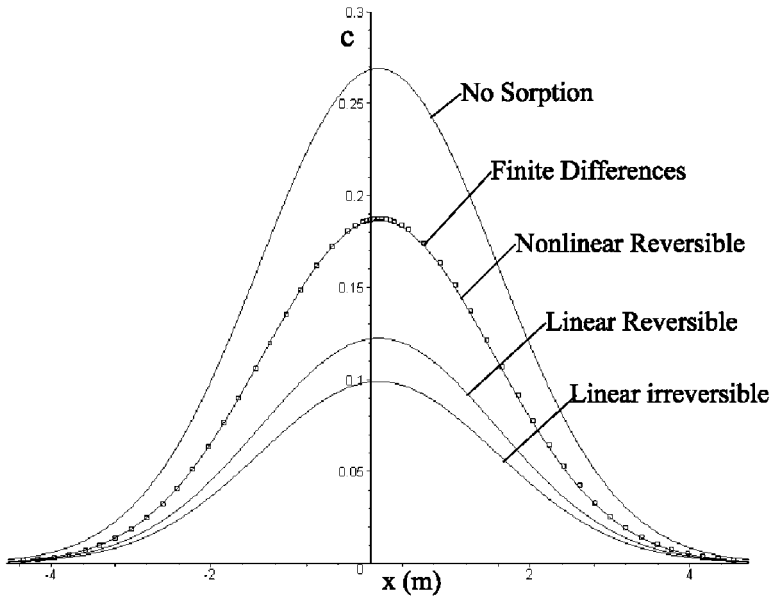

Figure 7. Concentration distribution according to reversible kinetic sorption models.

were verified with known limited exact solutions and with corresponding finite-difference solutions. Subsequently, simulations were conducted to study the effect of nonlinear reaction parameters on features of contaminant plumes after an instantaneous spill and after a symmetric initial condition. Features observed included the magnitude and spatial distribution of contaminant concentration, plume symmetry with respect to its center of mass, and the characteristics of back tails and sharp front ends. Comparison of nonlinear plumes with similar linear ones yielded a number of interesting observations which quantitatively explain field observations. In addition, the simple models developed may be used for groundwater pollution forecasting associated with monitoring and remedial actions, as well as parameter estimation of nonlinear plumes in the laboratory or in the field.

[20] The results indicated that nonlinear reactions may have a significant effect on the shape and spatial distribution of a contaminant at a given time, and in certain cases may explain quantitatively the occurrence of scaled, retarded, and nonsymmetric plumes, as well as the presence of back tails and sharp front ends usually observed in the field. By adopting a nonlinear model of contaminant migration a more realistic representation of contaminant propagation is possible than that obtained with a linear model.

[21] A plume traveling through an aquifer under irreversible nonlinear first-order kinetic sorption tends to preserve its symmetry with respect to its center of mass, but suffers a scaling with respect to a similar linear one. The degree of scaling is controlled by the magnitude of the nonlinear parameter b. Given a particular value of b, the

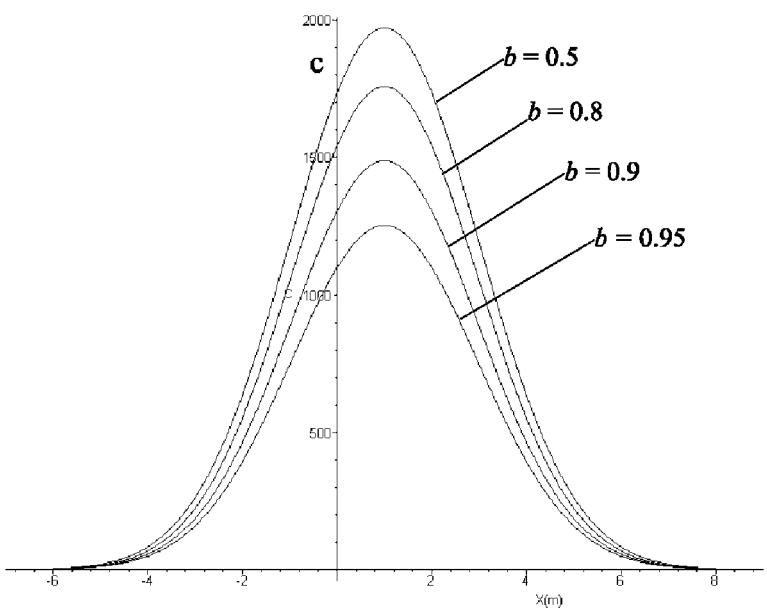

Figure 8. Effect of parameter b on contaminant distribution in a reversible nonlinear kinetic sorption model.

sense of scaling, either up or down with respect to the linear plume, is controlled by the position of the plume region in the solid-phase versus liquid-phase relationship. For values of $b < 1$, portions of the plume with liquid concentrations $c < 1$ experience a scaling down with respect to the linear one, whereas plume portions with $c > 1$ experience a scaling up with respect to the linear one. The opposite occurs when $b > 1$: portions of the plume with $c < 1$ experience a scaling up with respect to the linear plume, whereas portions of the plume with $c > 1$ experience a scaling down with respect to the linear one. Since a single plume, governed by a single value of b, may exhibit concentrations greater to or less than one at different locations, this would explain the occurrence of a rich variety of nonlinear plume shapes .

[22] A plume traveling under nonlinear Freundlich sorption loses its symmetry with respect of its center of mass thus resulting in a sharp front tail accompanied by a prolonged back tail. In addition, the Freundlich plume suffers retardation of the processes of advection and dispersion the degree of which is controlled by the magnitude of the nonlinear parameter b and by the position in the isotherm. When $b < 1$ and $c > 1$ the nonlinear plume suffers retardation of the processes of advection and dispersion, but not as severe as that of the linear sorption plume. This retardation reduces the velocity of the plume center of mass and the plume variance, the degree of which is controlled by the magnitude of b. The same observations related to nonlinear decay are applicable here. Therefore portions of the nonlinear plume with $c < 1$ suffer more sorption (i.e., more retardation, or less mobility) than that of the linear plume. When $b > 1$ and $c > 1$ the nonlinear plume suffers retardation of the processes of advection and dispersion that are more pronounced than that of the linear.

[23] In concert with a Freundlich model, a plume traveling under nonlinear Langmuir sorption experience a decrease in the velocity of the plume center of mass, and a corresponding increase in the magnitude of the maximum concentration with respect to the no sorption plume. This reduction in the center of mass, and corresponding increase in maximum concentration, is not as drastic as that of the linear plume. The Langmuir plume also exhibits the same nonsymmetrical features of the Freundlich.

[24] A plume traveling subject to reversible kinetic sorption experiences a partial contaminant return to the mobile phase, the degree of which is controlled by the magnitude of the backward constant relative to that of the forward constant. As the magnitude of the backward constant increases, the plume approaches the shape of the corresponding no-sorption one. Conversely, as the magnitude of this constant decreases, the plume approaches the shape of that of the linear sorption plume. If in addition, the forward reaction is nonlinear the shape of the plume may be significantly scaled. As before, the degree of plume scaling depends on the magnitude of the nonlinear parameter b. On the other hand, the direction of plume scaling, either up or down, is controlled by the position in which a particular plume region stands in the solid-phase liquid-phase relationship.

Appendix A: Decomposition of the Linear Dispersion Equation

[25] In this section we describe the basis of the method of decomposition applied to the linear dispersion equation. In particular, we show the details of the proof that the series equation (9), reproduced below as (A1), converges to (5), that is the exact solution to the linear advective-dispersive equation without decay.

A1. Theorem 1

[26] If the initial condition, $c_{00}(x)$, is piece-wise integrable in $(-\infty, +\infty)$, the decomposition series given by

$$c_0 = c_{00} + DL_t^{-1}\frac{\partial^2}{\partial x^2}\sum_{m=0}^{\infty} c_{0m} - uL_t^{-1}\frac{\partial}{\partial x}\sum_{m=0}^{\infty} c_{0m} \tag{A1}$$

converges to the exact solution (5) to the linear advective-dispersive equation with no decay.

A2. Proof

[27] Defining the transformed coordinates $\hat{x} = x - ut$, $\hat{t} = t$, and $v(\hat{x}, \hat{t}) = c_0(x, t)$, (A1) becomes

$$\begin{aligned} &v = f(\hat{x}) + DL_t^{-1}\frac{\partial^2}{\partial x^2}\sum_{m=0}^{\infty} v_m, \quad -\infty < \hat{x} < \infty, \quad 0 < \hat{t} \\ &v(\pm\infty, \hat{t}) = 0, \quad v(\hat{x}, 0) = c_{00}(\hat{x}) = f(\hat{x}) \end{aligned} \tag{A2}$$

From (A2), the first few terms in the series are:

$$\begin{aligned} v_0 &= f(\hat{x}) \\ v_1 &= L_t^{-1} D\frac{\partial^2 v_0}{\partial \hat{x}^2} = D\hat{t} f^{(ii)} \\ v_2 &= L_t^{-1} D\frac{\partial^2 v_1}{\partial \hat{x}^2} = \frac{(D\hat{t})^2}{2!} f^{(iv)} \\ &\vdots \end{aligned} \tag{A3}$$

or in short form,

$$v(\hat{x}, \hat{t}) = \sum_{n=0}^{\infty} \frac{(D\hat{t})^n f^{(2n)}}{n!} \tag{A4}$$

The Fourier transform of $v(\hat{x}, \hat{t})$ is given as

$$V(\lambda, \hat{t}) = \frac{1}{\sqrt{2\pi}} \int_{-\infty}^{\infty} e^{i\lambda\hat{x}} v\left(\hat{x}, \hat{t}\right) \mathrm{d}\hat{x}, \quad \mathrm{i} = \sqrt{-1} \tag{A5}$$

and the Fourier inversion formula as

$$v(\hat{x}, \hat{t}) = \frac{1}{\sqrt{2\pi}} \int_{-\infty}^{\infty} e^{-i\lambda\hat{x}} V(\lambda, \hat{t}) d\lambda \tag{A6}$$

Now define $V_0(\lambda, \hat{t})$ as the Fourier transform of $v_0(\hat{x}, \hat{t})$ in (A4), then from (A5)

$$V_0 = F(\lambda) = F(\lambda) = \frac{1}{\sqrt{2\pi}} \int_{-\infty}^{\infty} e^{i\lambda\hat{x}} f(\hat{x}) d\hat{x} \tag{A7}$$

Next, defining $V_1(\lambda, \hat{t})$ as the Fourier transform of $v_1(\hat{x}, \hat{t})$ in (A4) and using the rules of Fourier transforming derivatives,

$$V_1(\lambda, \hat{t}) = -D\lambda^2 \hat{t} F(\lambda) \tag{A8}$$

Similarly,

$$V_2(\lambda, \hat{t}) = \frac{(D\lambda^2 \hat{t})^2 F(\lambda)}{2!} \tag{A9}$$

Thus Fourier transforming the series (A4), and factorizing $F(\lambda)$, the resulting series $V_0 + V_1 + V_2 +$ may be written as

$$V(\lambda, \hat{t}) = F(\lambda)\left\{1 - D\lambda^2\hat{t} + \frac{\left(D\lambda^2\hat{t}\right)^2}{2!} - \frac{\left(D\lambda^2\hat{t}\right)^3}{3!} + \cdots\right\} \tag{A10}$$

which converges to

$$V(\lambda, \hat{t}) = F(\lambda) e^{-D\lambda^2 \hat{t}} \tag{A11}$$

After applying the Fourier inversion formula (A6), (A11) becomes

$$v(\hat{x}, \hat{t}) = \frac{1}{\sqrt{4\pi D\hat{t}}} \int_{-\infty}^{\infty} e^{-\frac{(\hat{x}-x')^2}{4D\hat{t}}} f(x') dx' \tag{A12}$$

Depending on the form of f, particular solutions may be obtained. For example, for $f(\hat{x}) = \delta(\hat{x})$ with $\delta(\ )$ the Dirac's delta function (i.e., an instantaneous spill of unit mass at the origin, (A12) reduces to

$$v(\hat{x}, \hat{t}) = \frac{e^{-\frac{\hat{x}^2}{4D\hat{t}}}}{\sqrt{4\pi D\hat{t}}} \tag{A13}$$

which is the fundamental solution, or Green's function, of the heat flow equation. In terms of concentration, after reverting to the original coordinates, (A12) becomes (5).

Appendix B: Decomposition of the Dispersion Equation Subject to Linear Decay

[28] In this section we show the details of the proof that the decomposition solution to equation (3), when $b = 1$ (i.e., linear decay) is (4). We use a different decomposition expansion that uses the semigroup operator associated with (3) [*Serrano*, 2001].

B1. Theorem 2

[29] If the initial condition to (3) is piece-wise integrable in $(-\infty, +\infty)$, the decomposition series generated by (3) when $b = 1$ converges to the exact solution (4).

B2. Proof

[30] Let us define the advective-dispersive differential operator as

$$L_{x,t} = \left(\frac{\partial}{\partial t} - D\frac{\partial^2}{\partial x^2} + u\frac{\partial}{\partial x}\right) \tag{B1}$$

(2) becomes

$$L_{x,t}c + \alpha c = 0 \tag{B2}$$

which maybe written as

$$c = -L_{x,t}^{-1}\alpha c \tag{B3}$$

where the inverse advective-dispersive operator, $L_{x,t}^{-1}$, is given by the convolution integral

$$L_{x,t}^{-1}\alpha c = \int_0^t J_{t-\tau} a c \, d\tau \tag{B4}$$

and the operator $J_t(\ )$ is the strongly continuous semigroup associated with (2) and it is given by [*Serrano*, 1996a]

$$J_t f = \frac{1}{\sqrt{4\pi D t}} \int_{-\infty}^{\infty} e^{-\frac{(x-ut-x')^2}{4Dt}} f \, dx' \tag{B5}$$

Now expand c in the right side of (B3) as the series $c = c_0 + c_1 + c_2 + \ldots$ From (B5) and (3), the first term in the series is equation (5):

$$c_0 = L_{x,t}^{-1}\frac{C_i\delta(x)}{\bar{C}} = \frac{C_i e^{-\frac{(x-ut)^2}{4Dt}}}{\bar{C}\sqrt{4\pi D t}} \tag{B6}$$

which is the fundamental solution or Green's function of the advective-dispersive equation. The second is

$$c_1 = -L_{x,t}^{-1} a c_0 = -\frac{atC_i e^{-\frac{(x-ut)^2}{4Dt}}}{\bar{C}\sqrt{4\pi D t}} \tag{B7}$$

The third term is

$$c_2 = -L_{x,t}^{-1} a c_1 = \frac{a^2t^2}{2}\frac{C_i e^{-\frac{(x-ut)^2}{4Dt}}}{\bar{C}\sqrt{4\pi D t}} \tag{B8}$$

In general, the nth term is given by

$$c_n = -L_{x,t}^{-1} a c_{n-1} = (-1)^n \frac{(at)^n}{n!}\frac{C_i e^{-\frac{(x-ut)^2}{4Dt}}}{\bar{C}\sqrt{4\pi D t}} \tag{B9}$$

Upon summation (4) follows.

Appendix C: Solving Nonlinear Equations With Decomposition

[31] Following the reviewers suggestion, I include some examples on the application of decomposition to the solution of nonlinear differential equations. For more details and examples, we refer the reader to *Adomian* [1994], and *Serrano* [2001, 1998]. To explain the essence of the method, consider initially a simple nonlinear differential equation given by

$$\frac{du}{dt} + au^2 = 0, \quad 0 < t, \quad u(0) = u_0 \tag{C1}$$

Using decomposition as before, we write the equation as

$$u = u_0 - aL_t^{-1}Nu, \quad Nu = u^2 \tag{C2}$$

where the nonlinear operator, N, is the term u^2. Let us expand the nonlinear term as an infinite series

$$u = u_0 - aL_t^{-1}\sum_{n=1}^{\infty} A_n \tag{C3}$$

Define the A_n as the Adomian polynomials given as a generalized Taylor series expansion about the initial term u_0:

$$\begin{aligned} A_0 &= Nu_0 = u_0^2 \\ u_1 &= -atL_t^{-1}A_0 = -atu_0^2 \\ A_1 &= u_1\frac{dNu_0}{du_0} = u_1u_0 = -2atu_0^3 \\ u_2 &= -aL_t^{-1}A_1 = a^2t^2u_0^2 \\ &\vdots \end{aligned} \tag{C5}$$

Alternative application of equations (C3) and (C4) produces, one by one, the terms in the series:

$$\begin{aligned} A_0 &= Nu_0 = u_0^2 \\ u_1 &= -atL_t^{-1}A_0 = -atu_0^2 \\ A_1 &= u_1\frac{dNu_0}{du_0} = u_1u_0 = -2atu_0^3 \\ u_2 &= -aL_t^{-1}A_1 = a^2t^2u_0^2 \\ &\vdots \end{aligned} \tag{C5}$$

Adding the terms, we observe that the resulting series converges to an exact closed form solution:

$$\begin{aligned} u &= u_0 + u_1 + u_2 + \dots \\ u &= u_0\left[1 - atu_0 + (atu_0)^2 - (atu_0)^3 + \dots\right] \\ u &= \frac{u_0}{1 + au_0t} \end{aligned} \tag{C6}$$

In this particular case, we were able to identify a closed form solution for the series. In many nonlinear equations, however, this is not possible and the modeler has to be content with the series themselves. The interesting feature is that one can calculate as many terms as one wishes in order to reach a desired level of accuracy. Thus modeling accuracy is the desired result, even though mathematical elegance is not always possible. The ith term requires knowledge of the term $(i - 1)$ or less, but not higher than that. This is an important feature of decomposition, as opposed to small perturbation schemes that require terms of order higher than i, with the unreasonable requirement of having to neglect the higher-order terms without any physical or mathematical basis other than a subjective declaration of "smallness."

[32] We offer here a different, more complex, nonlinear groundwater equation. Consider the Boussinesq equation subject to a time-dependent boundary condition given by

$$\begin{aligned} &\frac{\partial h}{\partial t} - \frac{1}{2}\frac{\partial^2 h^2}{\partial x^2} = 0, \quad 0 \le x \le 3, \quad 0 < t \\ &h(0,t) = h_b(t) = \frac{3}{2}\left(\frac{1}{(t+1)^{1/3}} - \frac{1}{t+1}\right) \\ &\frac{\partial h}{\partial x}(3,t) = 0, \quad h(x,0) = h_i(x) = x - \frac{x^2}{6} \end{aligned} \tag{C7}$$

where $h(x, t)$ is the hydraulic head; x is dimensionless distance; t is dimensionless time; $h_b(t)$ is a time-dependent left boundary condition; and $h_i(x)$ is the initial condition across the domain. A decomposition expansion of equation (C7) gives

$$h = h_0 + L_t^{-1}N(h) \tag{C8}$$

where the nonlinear operator

$$Nh = \frac{1}{2}\frac{\partial^2}{\partial x^2}(h_0 + h_1 + h_2 + \cdots)^2 = \frac{1}{2}\frac{\partial^2}{\partial x^2}\left(h_0^2 + 2h_0h_1 + h_1^2 + \cdots\right) \tag{C9}$$

From equations (C7), (C8), and (C9) each term in the series is calculated as

$$\begin{aligned} h_0 &= h_i \\ h_1 &= (1 - h_i)t \\ h_2 &= -(1 - h_i)t^2 - \frac{t^2}{6} \\ &\vdots \end{aligned} \tag{C10}$$

Upon summation, $h = h_0 + h_1 + h_2 + $, which converges to

$$h = \frac{h_i(x)}{(t+1)} + h_b(t) \tag{C11}$$

Equation (C11) is the exact solution to equation (C7) derived by *Sokolov* [1956] and reported by *Polibarinova-Kochina* [1977]. It satisfies the differential equation, the boundary and the initial conditions.

[33] **Acknowledgments.** The present work was supported by the National Science Foundation, grant number BCS-89-21004, and by research contract with HydroScience Inc., Lexington, Kentucky.

References

Abdulaban, A., J. L. Nieber, and D. Misra, Modeling plume behavior for nonlinearly sorbing solutes in saturated homogeneous porous Media, *Adv. Water Resour.*, *21*, 487–498, 1998.

Adomian, G., *Solving Frontier Problems in Physics-The Decomposition Method*, Kluwer Acad., Norwell, Mass., 1994.

Bolt, G. H., Movement of solutes in soils: Principles of adsorption/exchange chromatography, in *Soil Chemistry*, part B, *Physico-Chemical Models*, edited by G. H. Bolt, pp. 349–386, Elsevier Sci., New York, 1982.

Bosma, W. J. P., and S. E. A. T. M. Van der Zee, Analytical approximation for nonlinear adsorbing solute transport and first-order degradation, *Transp. Porous Media*, *11*, 33–43, 1993.

Boufadel, M. C., A mechanistic study of nonlinear solute transport in a groundwater-surface water system under state and transient hydraulic conditions, *Water Resour. Res.*, *36*(9), 2549–2565, 2000.

Fetter, C. W., *Contaminant Hydrogeology*, Macmillan, New York, 1993.

Khater, A. H., W. Malflietb, D. K. Callebautb, and E. S. Kamela, The tanh method, a simple transformation and exact analytical solutions for nonlinear reaction diffusion equations, *Chaos Solitons Fractals*, *14*(3), 513–522, 2002.

Liu, C., J. E. Szecsodya, J. M. Zacharaa, and W. P. Ballb, Use of the generalized integral transform method for solving equations of solute transport in porous media, *Adv. Water Resour.*, *23*(5), 483–492, 2000.

Perry, R. H., and D. W. Green, *Perry's Chemical Engineering Handbook*, McGraw-Hill, New York, 1997.

Polibarinova-Kochina, P. Y., *Theory of Groundwater Movement* (in Russian), Nauka, Moscow, 1977.

Serrano, S. E., Analytical solutions of the nonlinear groundwater flow equation in unconfined aquifers and the effect of heterogeneity, *Water Resour. Res.*, *31*(11), 2733–2742, 1995a.

Serrano, S. E., Forecasting scale dependent dispersion from spills in heterogeneous aquifers, *J. Hydrol.*, *169*, 151–169, 1995b.

Serrano, S. E., Towards a non-perturbation transport theory in heterogeneous aquifers, *Math. Geol.*, *28*(6), 701–721, 1996a.

Serrano, S. E., Hydrologic theory of dispersion in heterogeneous aquifers, *J. Hydrol. Eng.*, *1*(4), 144–151, 1996b.

Serrano, S. E., *Hydrology for Engineers, Geologists, and Environmental Professionals: An Integrated Treatment of Surface, Subsurface, and Contaminant Hydrology*, HydroScience, Lexington, K. Y., 1997.

Serrano, S. E., Analytical decomposition of the non-linear unsaturated flow equation, *Water Resour. Res.*, *34*(3), 397–407, 1998.

Serrano, S. E., *Engineering Uncertainty and Risk Analysis: A Balanced Approach to Probability, Statistics, Stochastic Modeling, and Stochastic Differential Equations*, HydroScience, Lexington, K. Y., 2001.

Serrano, S. E., and G. Adomian, New contributions to the solution of transport equations in porous media, *Math. Comput. Modell.*, *24*(4), 15–25, 1996.

Sheng, Q., and A. Q. M. Khaliqb, Modified arc-length adaptive algorithms for degenerate reaction diffusion equations, *Appl. Math. Comput.*, *126*(2–3), 279–297, 2002.

Simon, W., P. Reichert, and C. Hinz, Properties of exact and approximate traveling wave solutions for transport with nonlinear and nonequilibrium sorption, *Water Resour. Res.*, *33*(5), 1139–1147, 1997.

Sokolov, Y. D., On some particular solutions of the Boussinesq equation (in Russian), *Ukrainian Math. J.*, *8*, 48–54, 1956.

Van de Weerd, H., A. Leijnsel, and W. H. Van Riemsdijk, Transport of reactive colloids and contaminants in groundwater: effect of nonlinear kinetic interactions, *J. Contam. Hydrol.*, *32*(3–4), 313–331, 1998.

Van der Zee, S. E. A. T., Analytical traveling wave solutions for transport with non-linear and non-equilibrium adsorption, *Water Resour. Res.*, *26*(10), 2563–2578, 1990.

Van Genuchten, M. T., and R. Cleary, Movement of solutes in soils: Computer-simulated and laboratory results, in *Soil Chemistry*, part B, *Physico-Chemical Models*, edited by G. H. Bolt, pp. 349–386, Elsevier, New York, 1982.

Weber, W. J., P. M. McGuinley, and L. E. Katz, Sorption phenomena in subsurface systems: Concepts, models and effects on contaminant fate and transport, *Water Res.*, *25*(5), 499–528, 1991.

S. E. Serrano, Civil and Environmental Engineering Department, Temple University, 1947 N. 12th Street, Philadelphia, PA 19122, USA. (sserrano@temple.edu)